Simulation of damage mechanisms in high-speed grinding of structural ceramics

Philippe H. Geubelle and Spandan Maiti

Department of Aeronautical and Astronautical Engineering,
University of Illinois at Urbana-Champaign,
Urbana, IL 61801, USA

ABSTRACT

Due to the brittleness of ceramics, the machining of this class of materials is quite challenging. Assessing the surface and sub-surface damage associated with the machining process is of considerable interest nowadays. Most of the work in this area refers to the static indentation and/or scratch test. In this paper, we discuss an explicit grain-based cohesive-volumetric finite element scheme which can capture the complex dynamic initiation and propagation of intergranular cracks, near surface plasticity, and subsequent fragmentation of the material during dynamic scratch tests.

KEYWORDS

Ceramics, Dynamic fracture, Intergranular crack, Cohesive volumetric finite element, Grain-based meshing, Dynamic scratch test

INTRODUCTION

Many applications of advanced structural ceramics require high dimensional accuracy and surface finish, and, despite recent advances in the development of new surface finishing techniques such as electric discharge, laser beam and ultrasonic machining, conventional methods such as grinding, lapping and polishing [1] are still the common methods used in the industry. However, the brittleness of ceramics greatly increases the complexity of the grinding process, as the material removal process is often accompanied by surface and sub-surface damage in the form of cracks that sometimes penetrate deeply into the machined component. This residual damage can lead to substantial degradation of the mechanical strength, and hence the performance of the component [2,3]. Due to this added complexity, grinding alone accounts for 20 to 85% of the total cost of the machining process.

High-speed grinding, involving wheel rotation speed in excess of $20,000$ rpm and contact times in the $10...100$ μs range, is increasingly being considered not only to improve the productivity of machining process, but also as a way to reduce the amount of residual damage in the machined part [4]. However, the strain rates (in excess of $1000/s$) involved with such high speed of the machine tool render most of the existing analytical tools inadequate. Additional effects such as inertia, rate dependence, frictional heating and thermomechanical coupling must be taken into

account. Moreover, the existing analytical methods, mostly based on static continuum-level indentation solutions, are often oversimplified in their description of the complex interactions between various damage mechanisms taking place in the vicinity of the tool/specimen interface, and always involve a single grit system. Also, most of these analyses are performed at a macroscopic continuum level, disregarding the heterogeneous granular microstructure inherent to ceramic materials, and the complex propagation and branching paths of the cracks.

The objective of the research project described in this paper is the development and implementation of a numerical scheme aimed at the simulation of the complex damage process taking place during the high-speed machining of brittle materials that have a granular microstructure. In addition to the discrete microstructure of the material, emphasis is placed in this work on the capture of the inertial effects associated with high-strain rate loading, the spontaneous motion and interaction of cracks, and the complex interaction between the tool and the machined component. The numerical approach is based on an explicit, cohesive-based finite element scheme specially developed for the meso-scale level simulation of dynamic fracture in granular materials. The basic components of the numerical scheme are summarized in the next section.

Special emphasis is placed in this work on the simulation of the dynamic version of a common machinability test, the so-called *scratch test*, in which a single abrasive particle representing a

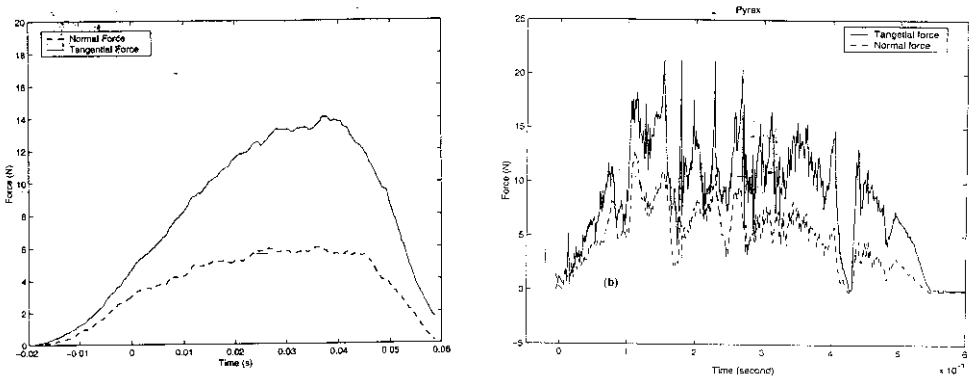

Figure 1: Experimental reaction trace at the base, a) for pyrex glass showing the brittle removal of material and a) for ASTM 1018 steel with much smoother curve signifying plastic flow of the material around the tool and b) for pyrex glass showing brittle removal of material [5].

single grit of the grinding wheel is scratched through the surface of the specimen for a prescribed length, allowing for the controlled study of the effect on the damage process of various parameters such as the depth of cut, the tool shape, the grit velocity and the material microstructure. The reaction trace at the base of the specimen obtained experimentally for the scratch test (Figure 1) shows the characteristic features for the brittle or plastic failure, with a smooth curve for the plastic case, and a curve with lots of spikes for the brittle one. A discussion of the simulation of these two tests is presented in the last section.

NUMERICAL SCHEME

The material removal process appearing in the grinding of ceramic materials has been shown to be associated with three distinct mechanisms: microfracture and chipping of individual grains, removal of large chunks of material by propagation of cracks parallel to the surface (referred to as lateral cracks), and intergranular microfracture and grain dislodgement. A small plastic

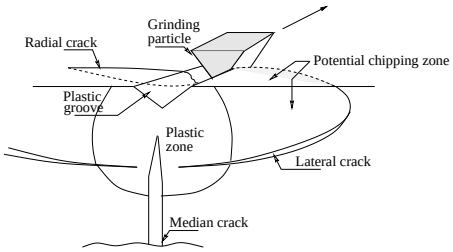

Figure 2: Scratch test of ceramic materials, showing the appearance of radial and lateral cracks and the formation of a plastic zone in the vicinity of grinding particle. (Adapted from [6]).

zone also develops in the vicinity of the surface. Special emphasis is placed in this work on the simulation of intergranular crack propagation and grain dislodgement, which have been shown to be dominant, especially at higher temperatures. In addition to assuming the intergranular nature of the process-induced cracks, we rely on two other important assumptions in the work described hereafter: the analysis is conducted in plane strain, and no thermomechanical coupling is so far considered. While these assumptions clearly limit the scope of the analysis, preventing for example, the study of the interaction between two parallel grits, we believe that the simplified model described hereafter captures the essential features of the physical problem.

Cohesive-based finite element scheme

To capture the spontaneous initiation, propagation, arrest and possible interaction of cracks in the specimen, we rely on a special form of the the cohesive-based finite element scheme, which has shown great success over the past few years in the capture of a variety of dynamic fracture problems [7,8,9]. The method relies on the combination of conventional (volumetric) elements used to capture the bulk response of the material, and interfacial (cohesive) elements used to simulate the spontaneous dynamic motion of intergranular cracks. The traction-separation law for the cohesive elements is taken to be bilinear [9]. According to this law, the relation between the normal (T_n) and tangential (T_t) cohesive tractions and the corresponding normalized displacement jumps ($\tilde{\Delta}_n$ and $\tilde{\Delta}_t$) takes the form

$$T_n = \frac{\mathcal{S}}{1-\mathcal{S}}\tilde{\Delta}_n \sigma_{max}, \qquad T_t = \frac{\mathcal{S}}{1-\mathcal{S}}\tilde{\Delta}_t \tau_{max}. \tag{1}$$

The normalized displacement jumps are defined as

$$\left\{ \begin{array}{c} \tilde{\Delta}_n \\ \tilde{\Delta}_t \end{array} \right\} = \left\{ \begin{array}{c} \Delta_n/\Delta_{nc} \\ \Delta_t/\Delta_{tc} \end{array} \right\}, \tag{2}$$

where

$$\tilde{\Delta}_{nc} = \frac{2G_{Ic}}{\sigma_{max}\mathcal{S}_{initial}}, \qquad \tilde{\Delta}_{nt} = \frac{2G_{IIc}}{\tau_{max}\mathcal{S}_{initial}}, \tag{3}$$

in which G_{Ic} and G_{IIc} are the critical energy release rates for mode I and mode II failures respectively, and $\mathcal{S}$ is the coupling factor between normal and tangential displacements and is a function of the norm of the displacement jump vector. Note that, the expression for T_n is only valid for the tension case. In compression, we always use the initial value of $\mathcal{S}$, which is close to unity, to generate a large compressive traction to ensure no overlapping between crack faces. This approach works well as long as the separation is small, and cohesive nodes maintain their initial connectivity. But after a large separation between initially adjacent nodes, this simple method cannot be used calling for more sophisticated contact detection and enforcement algorithms to prevent overlapping of newly created crack surfaces.

Grain-based mesh generation

Another critical aspect of this research is to capture the microstructure of the ceramic materials. Ceramic materials are essentially granular in nature. The cracks generally pass through grain boundaries generating a highly tortuous path. To capture the granular microstructure mentioned above, we use the Voronoi tessellation, a geometric structure with similar space-filling properties as the actual microstructure of the ceramics. The interior of Voronoi cells are further tessellated in Delaunay triangles, which act as volumetric elements in the finite element scheme. The nodes on the grain boundaries are doubled to generate the cohesive elements.

Explicit Elastic-Viscoplastic scheme

During grinding, grains can be subjected to large rotations and deformations, requiring the use of finite kinematics. Also, they can exhibit considerable plasticity. We assume the total deformation gradient admits a multiplicative decomposition into an elastic part $\boldsymbol{F}^e$ and a plastic part $\boldsymbol{F}^p$ [10] according to

$$\boldsymbol{F} = \boldsymbol{F}^e \boldsymbol{F}^p. \tag{4}$$

We compute $\boldsymbol{F}^{p^{-1}}$ iteratively through the relation

$$\left(\boldsymbol{F}^{p^{-1}}_{n+1}\right)_{ij} = (\boldsymbol{F}^{p^{-1}})_{ik}\left[\sum_A \frac{1}{\exp\left\{\frac{\Delta\gamma}{\sqrt{2\bar{\sigma}}}\sigma'^A\right\}}(\boldsymbol{N}^A)_k(\boldsymbol{N}^A)_j\right]. \tag{5}$$

The subscript n denotes the quantities in nth time step, whereas $n+1$ denotes the same for $(n+1)th$ time step. In this equation, $\Delta\gamma$ is the discretized plastic strain increment given by

$$\Delta\gamma = \Delta t\,\dot{\gamma}, \tag{6}$$

and the stress deviator $\boldsymbol{\sigma'}$ is defined as

$$\boldsymbol{\sigma'} = \sum_A (\boldsymbol{\sigma}^A - \frac{\boldsymbol{I}_1^\sigma}{3})\boldsymbol{n}^A \otimes \boldsymbol{n}^A. \tag{7}$$

The Lagrangian strain tensor $\boldsymbol{E}$ is related to second Piola-Kirchoff stress tensor $\boldsymbol{S}$ by the constitutive relation

$$\boldsymbol{S} = \boldsymbol{\mathcal{L}}\boldsymbol{E}, \tag{8}$$

where $\boldsymbol{\mathcal{L}}$ contains the elastic moduli of the material.

The finite element formulation used in the CVFE scheme is derived using principle of virtual work. An explicit central-difference time-stepping scheme [11] is used to calculate displacement $\boldsymbol{u}$, velocity $\dot{\boldsymbol{u}}$ and acceleration $\ddot{\boldsymbol{u}}$ at each time step.

Contact algorithm

The contact algorithm is necessary to enforce tool/grain and grain/grain contact. The algorithm has two major components: contact search and contact enforcement. The contact search is the most expensive part of the whole numerical scheme. To optimize it, we resort to a two-step search. The first step called the preliminary search quickly establishes the potential contact pairs. We take only the grains with at least one side broken as potential contact candidates. An axis-aligned rectangular bounding box is established around the grains/tool. The grains/tool with intersecting bounding boxes form the potential contact pair. In the next step, called the detailed search, only potential contact pairs are searched. An exhaustive search based on point-in-polygon principle is performed. For the contact enforcement, we resort to an explicit master/slave technique [12]. This technique is not particularly successful for closely packed grains with angular corners, as in our case. We are currently investigating other contact algorithms based on non-smooth contact dynamics. Coulomb friction is also taken into account.

RESULTS AND DISCUSSION

In the following example, the ceramic material is chosen as alumina (Young's modulus $E = 400\ GPa$, Poisson's ratio $\nu = 0.27$, and density $\rho = 3800\ kg/m^3$), whereas the tool is made of synthetic diamond (Young's modulus $E = 863\ GPa$, Poisson's ratio $\nu = 0.20$, and density $\rho = 3360\ kg/m^3$). The fracture toughness of the alumina in Mode I (K_{I_c}) as well as in Mode II are taken as 5.3 $MPa\sqrt{m}$, and maximum cohesive stress is chosen as 1/100th of the Young's modulus. The coefficient of friction is taken as 0.5.

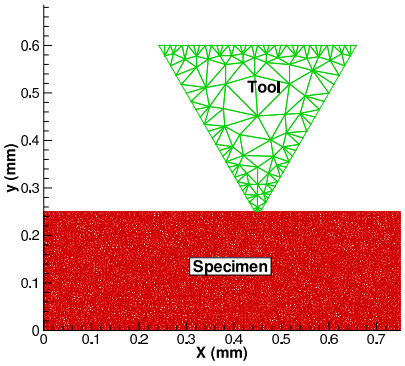

Figure 3: Finite element mesh for the scratch test simulation.

Figure 3 shows the typical meshing used for the problem with average grain size of 30 μm. The

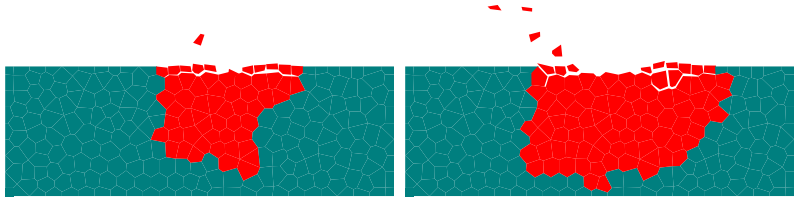

Figure 4: The deformed specimen at different time points for the brittle case : a) at time = 300×10^{-8} s, b)at time = 700×10^{-8} s. The darker region shows the damage zone.

horizontal velocity of the indenter is 66.66 m/s, whereas the vertical velocity varies linearly from 66.66 m/s to $-66.66\ m/s$. The ratio of yield stress to maximum cohesive stress, σ_y/σ_{max} is taken to be 1. Figure 4 shows snapshots of the material removal process. As can be seen from these pictures, we are able to capture the spontaneous initiation and the propagation of the intergranular cracks and grain dislodgement of the ceramic specimen. The normal reaction at the base (Figure 5a) shows the brittle nature of the damage process characterized by sharply discontinuous peaks and oscillations in the reaction trace. The same system is studied for a more ductile system with $\sigma_y/\sigma_{max} = 5$. Figure 5b depicts the normal bottom reaction for this problem. It can be seen that, at the beginning, the failure process is ductile, and reaction curve is smooth. But, as the strain rate increases, the yield stress increases also, ultimately transforming the failure process to a brittle one.

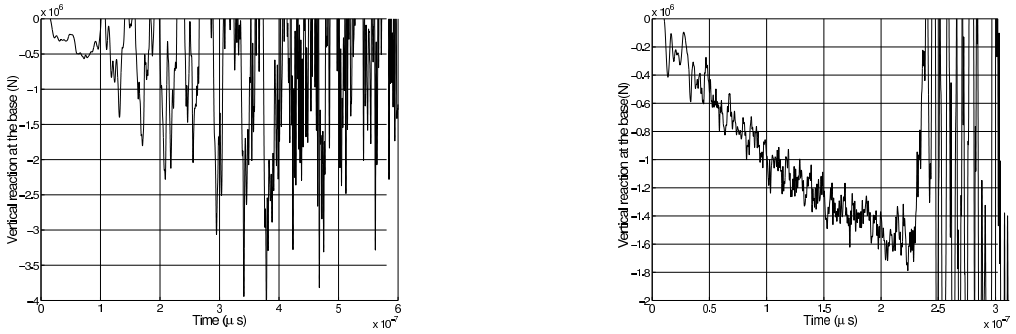

Figure 5: The vertical reactions at the base of the specimen for the scratch test : a) for the brittle case, $\sigma_y/\sigma_{max} = 1$, b) for the ductile case, $\sigma_y/\sigma_{max} = 5$.

Conclusions

In this paper, we have shown the capability of our model to capture the dynamic crack growth with an emphasis on the granular microstructure of the ceramic material. The model can capture the brittle and ductile failure process associated with high strain rate. Detailed analyses are underway to characterize the effects of tool velocity and trajectory on the damage process.

Acknowledgements

This research project is funded by NSF through the Career Award CMS-9734473.

References

1. Klocke, F. (1996) *J. Eur. Ceram. Soc.* 17, 457.
2. Liu, D. M., Fu, C. T. and Lin, L. J. (1996) *Ceramic Int.* 22, 267.
3. Esposito, L., Tucci, A. and Andalo, G. (1997) *J. Eur. Ceram. Soc.* 17, 479.
4. Malkin, S. and Ritter, J. E. (1989) *J. Eng. Ind.* 111, 167.
5. Subhash, G., Loukus J. E. and Pandit, S. M. (2001). In preparation.
6. Li, K. and Liao, T. W. (1996) *J. Mat. Proc. Techn.* 57, 207.
7. Camacho, C. and Ortiz, M. (1996) *Int. J. Solids Struct.* 33, 2899.
8. Xu, X.-P. and Needleman, A. (1994) *J. Mech. Phys. Solids* 42, 1397.
9. Geubelle, P. H. and Baylor, J. (1998) *Comp. B* 29, 589.
10. Simo, J. C. (1988) *Comp. Meth. Appl. Mech. Engr.* 66, 199.
11. Belytschko, T., Chiapetta, R. L. and Bartel H. D. (1976) *Int. J. Numer. Meth. Eng.* 10, 579.
12. Taylor, L. and Flanagan, D. (1987). Report SAND86-0584, Sandia National Laboratories, Albuquerque.